Functional Characterization of *Anopheles* Matrix Metalloprotease 1 Reveals Its Agonistic Role during Sporogonic Development of Malaria Parasites

Evi Goulielmaki,[a,b] I. Sidén-Kiamos,[a] Thanasis G. Loukeris[a]†

Institute of Molecular Biology and Biotechnology, Foundation of Research and Technology-Hellas, Heraklion, Crete, Greece[a]; Biology Department, University of Crete, Heraklion, Crete, Greece[b]

The ability to invade tissues is a unique characteristic of the malaria stages that develop/differentiate within the mosquitoes (ookinetes and sporozoites). On the other hand, tissue invasion by many pathogens has often been associated with increased matrix metalloprotease (MMP) activity in the invaded tissues. By employing cell biology and reverse genetics, we studied the expression and explored putative functions of one of the three MMPs encoded in the genome of the malaria vector *Anopheles gambiae*, namely, the *Anopheles gambiae MMP1* (*AgMMP1*) gene, during the processes of blood digestion, midgut epithelium invasion by *Plasmodium* ookinetes, and oocyst development. We show that AgMMP1 exists in two alternative isoforms resulting from alternative splicing; one secreted (S-MMP1) and associated with hemocytes, and one membrane type (MT-MMP1) enriched in the cell attachment sites of the midgut epithelium. MT-MMP1 showed a remarkable response to ookinete midgut invasion manifested by increased expression, enhanced zymogen maturation, and subcellular redistribution, all indicative of an implication in the midgut epithelial healing that accompanies ookinete invasion. Importantly, RNA interference (RNAi)-mediated silencing of the *AgMMP1* gene revealed a postinvasion protective function of AgMMP1 during oocyst development. The combined results link for the first time an MMP with vector competence and mosquito-*Plasmodium* interactions.

Matrix metalloproteases (MMPs) (metzincin clan of metallopeptidases) have been identified in a wide range of organisms from bacteria (1–3) and viruses (4) to humans. The multitude of individual MMP genes varies significantly among different multicellular organisms. Twenty-four distinct MMP genes are present in the human genome, while in contrast, a limited number of MMPs is predicted in the sequenced arthropod genomes. Two MMPs are encoded in the fruit fly *Drosophila melanogaster* genome (5, 6) and three in the beetle *Tribolium castaneum* genome (7) and the malaria vector *Anopheles gambiae* genome.

In general, expression of MMP genes is regulated through complex transcriptional circuits governing the levels, tissue/cell type pattern, and/or response to different stimuli (8). In mammals, some MMP members (including several membrane type MMPs [MT-MMPs]) are expressed constitutively, implying a role in tissue homeostasis, however, most MMPs are transcriptionally induced particularly during tissue repair or remodeling, as well as in diverse disease states and inflammation (9). Removal of the autoinhibitory prodomain by limited proteolysis is the main way for MMP activation. A subgroup of MMPs (including all MT-MMPs) is activated by endoplasmic reticulum (ER)-resident proprotein convertases (e.g., furin); however, most MMPs are secreted as inactive precursors (also known as zymogens), and their activation in the extracellular/pericellular space requires limited proteolysis or chemical modification of the prodomain Cys switch (9, 10). Upon their conversion into active enzymes, MMPs are controlled by specialized inhibitors, namely, the tissue inhibitors of metalloproteases (TIMPs) or the more general α_2-macroglobulin inhibitor (11).

MMPs were initially identified as the enzymes that degrade extracellular matrix (ECM) components (12, 13) and/or process molecules that mediate cell-cell and cell-ECM interactions (14–16). As a result of MMP-mediated proteolysis, cells are enabled to glide over ECM (17) or to infiltrate tissues (18, 19). More recently, genetic studies of individual MMPs and high-throughput proteomic analyses in mammals (20, 21) revealed novel MMP substrates expanding the functional roles of MMPs. Among the well-established developmental functions of MMPs are included the promotion of cell proliferation, survival, and differentiation (22, 23), achieved through the activation of latent growth factors (23), or through the generation of growth-promoting peptides (matrikines) derived as proteolytic by-products of ECM components (22, 24).

Drosophila's powerful genetics and the limited number of MMP genes in this model species have enabled elegant genetic studies considerably advancing our knowledge regarding the functional implication of MMPs in processes such as tissue remodeling during developmental transitions (25–27), cell fate/identity determination (28, 29), and neuron axon path finding (30). Moreover, arthropod MMPs were shown to be actively involved in wound healing (31, 32).

Microbial metalloprotease activity has been shown to elicit immune responses (33). In parallel, host MMPs also exert agonistic

and antagonistic forces over pathogens promoting or dampening inflammation and responses of the innate immune system (34), i.e., through the activation of antimicrobial peptides (alpha and beta defensins) (35) and/or by activation or deactivation of cytokines (36), chemokines (37), and chemokine receptors (38).

In the moth *Galleria mellonella*, lipopolysaccharide (LPS) challenge induces *G. mellonella MMP1* (*GmMMP1*) transcription in hemocytes and triggers MMP-dependent degradation of collagen IV (39), whereas in *Tribolium*, silencing of *MMP1* results in higher susceptibility to the entomopathogenic fungus *Beauveria bassiana* (7). MMP activity is also induced by the insect baculovirus, *Autographa californica*, in the midgut of *Trichoplusia ni*, facilitating the escape and spreading of the virus through the tracheal system and promoting systemic infections (40). Finally, in *Drosophila*, overexpression of an activated matrix metalloprotease 2 (MMP2) in the fat body triggers the immune deficiency (IMD) pathway (41) responsible for the Gram-negative antibacterial responses.

Despite their intriguing implications in tissue invasion by pathogens, tissue repair, and innate immunity, MMPs have been overlooked in disease vector mosquitoes so far. Nevertheless, on the basis of our current knowledge, one might hypothesize a potential involvement of MMP activity at different points in the course of the malaria parasite life cycle within the mosquito. In the present study, we characterize in detail one of the three MMPs encoded in the *Anopheles gambiae* genome, namely, *A. gambiae MMP1* (*AgMMP1*). We show that *AgMMP1* manifests a complex gene expression pattern (involving alternative splicing) and regulation at multiple levels. By employing cell biology and reverse genetics, we expose potential implications of the *AgMMP1* protein products during the midgut epithelial healing that follows invasion by *Plasmodium berghei* ookinetes, and most importantly during *P. berghei* oocyst development. Thus, our study indicates a potential impact of MMPs in vector competence determination. Moreover, we demonstrate the utility of *Anopheles/Plasmodium* as an experimental model to study the complex molecular regulation of this particular group of multifunctional proteases.

MATERIALS AND METHODS

Ethics statement. Animal-related work has passed through an ethical review process/approval by the Foundation for Research & Technology (FORTH) Ethics Committee (FEC) and was carried out in certified animal facilities by trained personnel (license code of Veterinary Services EL91BIO02). All work was conducted in accordance with the Presidential Decree (PD) 160/1991 that harmonizes national legislation with the EC Directive 1986/609 and Law 2015/2001 on vertebrate animals used for research and other scientific purposes.

Mosquito cultures and parasite infection. *Anopheles gambiae* G3 strain was maintained under standard conditions. *Plasmodium berghei* 507 cl1strain, expressing green fluorescent protein (GFP) throughout the life cycle (42), was primarily used in mosquito infections following standard procedures.

Cells and transfections. *A. gambiae* Sua 4.0 cells were cultured as described previously (43). For plasmid transfections, approximately 3 × 10^6 cells were seeded in 3 ml culture medium in a 6-well plate and allowed to attach. The cells were transfected with 4 μg total plasmid DNA using Effectene reagent according to the manufacturer's instructions and as described in reference 44. In general, the cells were incubated for 36 h with the transfection mixture and subsequently were placed in serum-free medium for 24 h prior to their harvesting for analysis. In the case of activated MT-MMP1 proteolysis inhibition, the broad-spectrum MMP inhibitor GM6001 was added to the serum-free medium at a final concentration of 100 μM. In the cotransfection experiments, the following plasmid mix-

tures were used: (i) actin-tTA2s (tTA stands for transcriptional *trans*-activator) (1 μg), tetOP-GFP (transfection control plasmid) (1 μg), and tetOP-aMT-MMP1 (aMT stands for "activated" MT) (2 μg) and (ii) actin-tTA2s (1 μg), tetOP-GFP (1 μg), tetOP-aMT-MMP1 (1 μg), and TetOP-TIMP (1 μg). For gene silencing, 3 μg of each double-stranded RNA (dsRNA) was transfected into a confluent culture (6-well plate) using the Effectene transfection reagent as described in reference 45; 24 to 36 h later, the medium was exchanged with fresh, serum-free medium, and the cells and supernatants were harvested 24 h later.

RNA expression analysis. For expression profiling, total RNA was prepared from carcasses and midguts, and from infected and naive-blood-fed midguts at different time points after feeding. For validating gene silencing, total RNA was prepared from dsRNA-treated mosquitoes 24 h postfeeding (PF) (and 3 to 4 days after dsRNA injection). In all cases, RNAs were prepared using the TRIzol reagent (Invitrogen), and reverse transcription was performed with Moloney murine leukemia virus (MMLV) reverse transcriptase (Invitrogen) following standard procedures.

Real-time quantitative reverse transcription-PCR (qRT-PCR). Amplifications were performed in the presence of SYBR green dye. All reactions were analyzed using the ABI PRISM 7700 sequence detection system following the manufacturer's instructions (Applied Biosystems, Foster City, CA, USA). Expression levels were calculated by the relative standard curve method (46), using (i) *S7* as an endogenous gene reference and (ii) calibrators appropriate to each experiment (e.g., expression levels of *A. gambiae MMP1* [*AgMMP1*] and/or *A. gambiae TIMP* [*AgTIMP*] at the time point MPF [a few minutes postfeeding]; or expression levels of *AgMMP1*, *AgMMP2*, and *AgTIMP* transcripts in the midguts of *dsGFP*-treated mosquitoes). Serial dilutions (1 to 1,000 pg) of plasmids containing either *AgMMP1*, *AgTIMP*, *AgMMP2*, or *S7* sequences were used in each run to perform standard curve analysis. Gene-specific primers were designed with the Oligo software taking care to span intron-exon boundaries (rtMMP1FW [rt stands for reverse transcription, and FW stands for forward] [TCTCTGGGTCTGACTCACTCGG], rtMMP1Rev [Rev stands for reverse] [GCGTTGAATGCCCTGAATA], rtMMP2FW [TGGTCGACTCTACTGGAAATTC], rtMMP2Rev [GCCCTTGAAGAAGTACGTCT], rtTIMPFW [GGATGGTGATGCTTCCCAC], rtTIMPRev [CAACACTTGTGCAACGATTACG], rtS7FW [GTGCGCGAGTTGGAGAAGA], and rtS7Rev [ATCGGTTTGGGCAGAATGC]).

Semiquantitative reverse transcription-PCR. Amplifications were performed with the following set of primers: AgMMP2For (For stands for forward) (GAGTTGGATGCGGGACAGGTC), AgMMP2 Rev (TGCGCGGTCCATAGATCGATT), AgTIMP For (GGATGCGTACAAGATTGCAATC), AgTIMP Rev (TCACGGGTACTTGGGACTATT), AgMMP1 For (CAACATCGATGCCGCGTTTAC), and AgMMP1Rev (TCGACGGTGTGTTCTTGCAGC). S7 was used as an endogenous gene reference as described above. The standard program comprised a cycle of 5 min at 95°C, 30 s at 58°C, and 30 s at 72°C. The appropriate number of cycles was selected so that the amplification of the transcript would be exponential and the product would be clearly visible on an agarose gel (see below) in order to be quantified. The PCR products were loaded onto SYBR green-stained agarose gels. Images of the SYBR green-stained agarose gels were acquired with a Cohu high-performance charge-coupled-device (CCD) camera (Cohu Inc., San Diego, CA), and quantification of the bands was performed by Phoretix 1 D (Phoretix International Ltd., Newcastle upon Tyne, United Kingdom). Band intensity was expressed as relative absorbance units. Data presented are normalized to S7 expression.

Isolation of MT-MMP1 and secreted MMP1 (S-MMP1) encoding cDNAs. *Anopheles* expressed sequence tag (EST) database (http://web.bioinformatics.ic.ac.uk/vectorbase/AnoEST.v8) revealed two EST clones (accession numbers BM617134 and NAP1-P117-H-04) encoding a different cDNA sequence matching the 3′ prime end of the MMP1 gene (Anobase accession number AGAP006904) than the one initially predicted. Based on the above, two alternative reverse primers were designed (REVMMP1iso1 and REVMMP1iso2) and in combination with a com-

mon forward primer (FWMMP1; hybridizing at the area of the initiator ATG) were used to amplify the two alternative MMP1 cDNAs from carcass cDNA (FWMMP1 [ATGCTACGCAATCACGCACAC], REVMMP1iso1 [CTAGCAGCGGCTGACAAGGTA], and REVMMP1iso2 [TTACAGAGAGTTGCGACGAAC]). Amplified PCR products were subcloned in TOPO_TA vector and sequence verified.

tetOP-aMT-MMP1 and tetOP-TIMP plasmid constructions. The cDNA encoding a truncated MT-MMP1 version from which were excluded the sequences encoding the endogenous signal peptide and the prodomain were amplified by PCR using appropriately designed primers and were incorporated in the tetOPLink plasmid (S. Kaforou and T. G. Loukeris, unpublished data), fused at the 5′ end with sequences encoding a1 antitrypsin signal sequence (a1AT) and a three-myc epitope tag (3xmyc). The cDNA encoding the whole open reading frame (ORF) of AgTIMP was also amplified using appropriate primers and inserted in the tetOPLink. The primers used were as follows (restriction sites are underlined): FWaMT-MMP1 (AAACATATGCTGCAGGGCAGCCGCTGGAAG), REVaMTMMP1 (GGCTCGAGCTAGCAGCGGCTGACAAGGTA), FWTIMP (GAATTCATGAAGACGAACCGTCTGCTA), and REVTIMP (GAATTCTCACGGGTACTTGGGACTATT).

dsRNA production and mosquito treatment. For the production of dsRNAs, the following plasmids were used: pLL10GFP (gift of E. Levashina, Department of Vector Biology, Max Planck Institute for Infection Biology, Berlin, Germany), pLL10MMP1, pLL10TIMP, and pLL10MMP2. For the construction of pLL10MMP1 and pLL10MMP2, an *AgMMP1* and *AgMMP2* cDNA fragment (1049 bp to 1500 bp of the MMP1 cDNA and 312 bp to 720 bp of the MMP2 cDNA) were amplified using the following primers: dsMMP1FW (CAACATCGATGCCGCGTTTAC), dsMMP1REV (TCGACGGTGTGTTCTTGCAGC), dsMMP2FW (GAGTTGGATGCGGGACAGGTC), and dsMMMP2REV (TGCGCGGTCCATAGATCGATT).

For the construction of pLL10TIMP, the whole *AgTIMP* cDNA was amplified using primers dsTIMPFW (GGATGCGTACAAGATTGCAATC) and dsTIMPREV (TCACGGGTACTTGGGACTATT). In both cases, the amplified products were subcloned into the EcoRI site of pLL10 (47). dsRNAs using the above plasmids as the templates were produced as described previously (47); mosquitoes were injected with 600 ng of *AgMMP1*, *AgTIMP*, *AgMMP2*, or control *GFP* dsRNA as described in reference 47. *Plasmodium berghei* infections were performed 3 days postinjection. Midguts were dissected 2 or 7 days postinfection, and oocyst numbers were counted using a fluorescence microscope.

Antibody production. The C-terminal sequence of *AgMMP1* cDNA corresponding to the hinge region and the three hemopexin domains was amplified and inserted into plasmid pET-16b in fusion with the His tag. The sequence encoding the inhibitory domain of *AgTIMP* was cloned in the same vector. The recombinant antigens were produced in *Escherichia coli* strain BL21(DE3)pLysS. Nickel affinity chromatography was used to purify the antigens that were used to raise the respective polyclonal rabbit sera. The derived positive sera were affinity purified against the recombinant antigens. The primers used for cloning of *AgMMP1* and *AgTIMP* fragment were as follows: AgMMP1AgFW (AAACATATGGACGTACGATCGGCACTGATG), AgMMP1AgREV (AAAGGATCCTCATAGCGCGGCATCGACACT), AgNTIMPFor (AAACATATGTGCAGCTGCCTCCCGCAGCAT), and AgNTIMPRev (AAAGGATCCTCAGCCCTTGCGATAGACGCCG).

Immunofluorescence. Mosquito midgut epithelial sheets were prepared for an immunofluorescence assay (IFA) as described elsewhere (48, 49), while circulating hemocytes were collected and prepared as described in reference 48. Samples were incubated with purified anti-AgMMP1 purified serum (1:300), anti-P28 monoclonal antibody (1:1,000), anti-PbCap380 serum (1:1,000) (50), anti-integrin serum (1:1,000) (51). The following secondary antibodies were used: Alexa Fluor 568-labeled goat anti-rabbit IgG, 1:1,000; Alexa Fluor 488-labeled goat anti-mouse IgG, 1:1,000. Actin and nuclei were stained with Phalloidin 488 (1:100) and TO-PRO (diluted 1:1,000 in the case of midgut epithelial sheets stain-

ing; 1:500 in the case of hemocytes). Samples were analyzed by using a Bio-Rad confocal microscope.

Western blot analysis, zymography, and densitometry. The equivalent of 5 to 10 midguts was loaded per lane in the case of midgut Western analysis, while in the case of hemolymph, extracts were loaded at approximately the equivalent of 15 to 20 mosquitoes per lane. Hemolymph extracts were quantitated by the Bradford assay before loading. For Western analysis of *A. gambiae* Sua 4.0 cells, the cell pellet (CP) was separated from the culture medium (CM) by centrifugation. CP proteins were extracted using radioimmunoprecipitation assay (RIPA) buffer and repeated cycles of freeze-thaw. CM proteins were precipitated with acetone. Approximately one-fourth of CP or CM deriving from one well (9.5 cm²) was loaded per lane. In the case of CP Western blots, the membranes were stripped and reincubated with anti-GFP antibody as a transfection/loading control. Antibodies used in Western blots were as follows: purified anti-AgMMP1 (1:500), purified anti-AgTIMP (1:100), anti-GFP (1:1,000; Minotech), anti-myc (1:10,000; Cell Signaling), and antitubulin (1:1,000; Abcam). Secondary antibodies used were horseradish peroxidase (HRP)-linked anti-rabbit IgG (1:10,000) and HRP-linked anti-mouse IgG (1:10,000). For casein zymography, protein samples were resolved on 12% SDS-polyacrylamide gels containing 1 mg/ml casein, and the whole procedure was performed as described in reference 6.

Following chemiluminescence, Western blot signals were analyzed using ImageJ software to determine relative band intensities and calculate quantitative differences of AgMMP1 expression.

RESULTS

The *Anopheles gambiae MMP1* gene encodes two alternative isoforms with different tissue distributions. Most MMPs are defined by a common evolutionarily conserved structural architecture that includes the signal sequence, an autoinhibitory prodomain identified by a conserved Cys residue (also known as the Cys switch), and a catalytic domain linked through a hinge region to a variable number of hemopexin domains. Depending on the existence of a transmembrane domain and/or of glycosylphosphatidylinositol (GPI)-anchoring signals, MMPs are classified into secreted and membrane type MMPs (9, 11).

The annotated *Anopheles gambiae* genome includes three genes, predicted to encode proteins possessing the above molecular architecture. In accordance with their relative homologies with the MMPs of *Drosophila* and *Tribolium*, the genes were named *AgMMP1* (AGAP006904), *AgMMP2* (AGAP011870), and *AgMMP3* (AGAP003929). Preliminary expression profiling showed that *AgMMP1* was almost equally expressed in the adult female midguts and carcasses, in contrast to *AgMMP2* and *AgMMP3*, which were expressed more abundantly in carcasses (see Fig. S1 in the supplemental material). Transcripts of the only tissue inhibitor of metalloproteases (*AgTIMP*) encoded in the *Anopheles* genome were equally distributed between midguts and carcasses (Fig. S1).

Our searches in the *Anopheles gambiae* EST database revealed the presence of two alternative ESTs matching the 3′ end of *AgMMP1*. We used a combination of a common and EST-specific primers to amplify, from carcass mRNA, cDNAs corresponding to the two alternative transcripts. One of the recovered cDNAs encoded a 571-amino-acid (aa) transmembrane protein and was thus named MT-MMP1. The second cDNA encoded a slightly shorter protein of 539 amino acids, lacking the transmembrane domain, thus corresponding to a secreted AgMMP1 isoform (S-MMP1) (Fig. 1A). Apart from this difference, MT-MMP1 and S-MMP1 share the same molecular architecture, including three identical hemopexin domains (HPDs) and a furin/proprotein
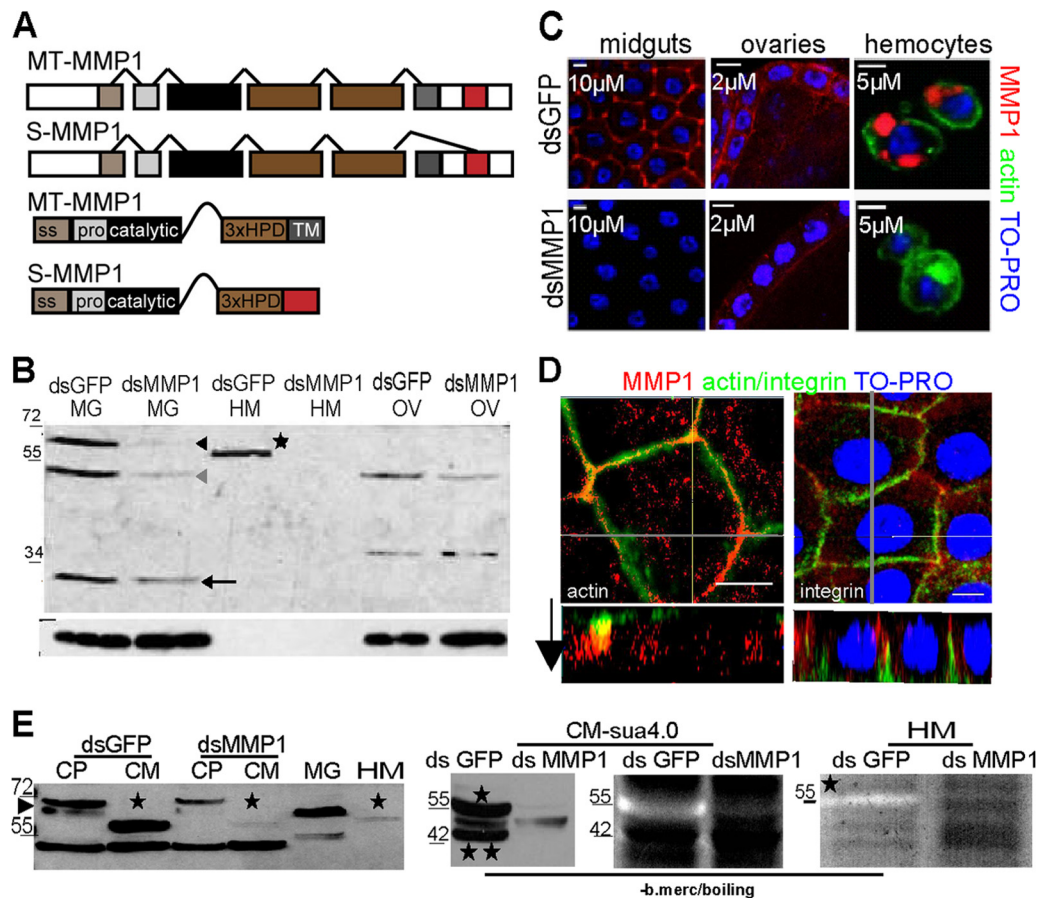
FIG 1 AgMMP1 is expressed as two alternative isoforms. (A) Exon/intron organization of the two alternative *Anopheles AgMMP1* transcripts and the predicted domain organization of the encoded proteins; alternative splicing takes place in the last exon excluding the sequence encoding a transmembrane region (TM) from the *S-MMP1* isoform. SS, signal sequence; pro, prodomains; 3xHPD, three hemopexin domains. (B, top) Western blot analysis of extracts from isolated tissues (midgut [MG], hemolymph [HM], and ovaries [OV]), derived from either *dsMMP1*- or *dsGFP* (control)-treated, blood-fed female mosquitoes, probed with anti-AgMMP1 purified serum. The black and gray arrowheads indicate the positions of MT-MMP1 precursor (zymogen) and active protease, respectively, whereas the black arrow marks the positions of a putative proteolytic product of low molecular weight that is occasionally detected in MG extracts. The black star marks the position of precursor S-MMP1; tubulin was used for sample normalization of MG and OV extracts (bottom blot). In the case of HM extracts, normalization was performed by the Bradford assay prior to loading (~70 μg). The positions of molecular mass markers (in kilodaltons) are indicated to the left of the gel. (C) IFAs of midgut epithelia, female ovaries, and peripheral hemocytes derived from *dsMMP1*- and/or *dsGFP*-treated, blood-fed female mosquitoes stained with anti-AgMMP1 purified serum (red), phalloidin (green), or TO-PRO (blue). (D) Stacks of horizontal optical sections of midguts derived from naive-blood-fed female mosquitoes. *x-z* optical projections of each section (perpendicular to the gray lines) are shown in the bottom panels. The arrow indicates the orientation of the epithelium (apical to basal). (Left) The epithelium is stained with anti-AgMMP1 (red) and phalloidin (green). (Right) The epithelium is stained with anti-AgMMP1 (red) and anti-integrin beta subunit (green). Bars, 10 μm. (E, left) Western analysis of total protein extracts from cell pellet (CP) and culture medium (CM) of Sua 4.0 cells pretreated with either *AgMMP1* or *GFP* (control)-specific dsRNA. Extracts from mosquito midguts (MG) and hemolymph (HM) are also included as positive controls. The position of precursor S-MMP1 is indicated with a black star, while the black arrowhead indicates the position of precursor MT-MMP1, traces of which are detected in the CP. (Middle right) Casein zymography of CM samples derived from Sua 4.0 cells pretreated with dsRNA specific for either *AgMMP1* or *GFP* (control); (middle left) Western analysis with the anti-AgMMP1 purified serum of the same samples used in zymography. The position of precursor S-MMP1 is indicated by a single black star, while the position of a putative S-MMP1 active form is indicated by a pair of black stars. (Right) Zymographs of HM extracts derived from *dsMMP1*- and *dsGFP*-treated, blood-fed female mosquitoes. The black star indicates again the position of precursor S-MMP1. Zymography and Western blotting indicated were performed without β-mercaptoethanol and without boiling.

convertase (PC) cleavage site between the prodomain and the catalytic domain.

In order to reveal the tissue/cell type distribution of the AgMMP1 isoforms, a serum was raised, using as an antigen a bacterially produced peptide that included the hinge region and the three HPDs. The serum was affinity purified against the antigen and used to analyze by Western blotting, extracts from different tissues (midguts, ovaries, and hemolymph) dissected from blood-fed female mosquitoes pretreated with *GFP*-specific dsRNA (*dsGFP*). Extracts of the same tissues dissected from mos-

quitoes pretreated with *AgMMP1*-specific dsRNA (*dsMMP1*) were analyzed in parallel (Fig. 1B, top panel).

Two AgMMP1-related bands of ~63 and 50 kDa (Fig. 1B, black and gray arrowheads) were predominantly detected in midgut extracts derived from *dsGFP*-pretreated mosquitoes, together with an additional ~34-kDa minor band (black arrow), the presence of which varied between experiments. The ~50-kDa band was also predominant in extracts derived from dissected ovaries. Instead, an AgMMP1-related band of ~55 kDa was detected exclusively in the hemolymph extract (black star). The in-

tensity of all the above bands was drastically reduced in the similarly prepared midgut extracts from *dsMMP1*-pretreated mosquitoes, indicating that they are all *AgMMP1* derivatives. According to the protein mass predictions, the 63- and 50-kDa bands correspond, respectively, to the zymogen and the active forms of MT-MMP1, while the 55-kDa band possibly corresponds to the zymogen form of S-MMP1. Casein zymography performed in parallel revealed a lytic band of the size expected for the zymogen S-MMP1 in the hemolymph extracts of *dsGFP*-pretreated mosquitoes that was absent from similarly analyzed extracts derived from *dsMMP1*-pretreated mosquitoes (Fig. 1E, rightmost panel).

The purified anti-AgMMP1 serum was used in immunofluorescence assays (IFAs) of midguts, ovaries, and hemocytes. Intense AgMMP1 staining decorated the cell attachment sites in the midgut and follicular epithelia (Fig. 1C), while in isolated peripheral hemocytes, AgMMP1 immunoreactive material accumulated within large intracellular vesicles (Fig. 1C). Midgut epithelial sheets were in addition stained with the AgMMP1 serum in combination with either an integrin-specific serum, or phalloidin. Integrin marks the basal side of the midgut epithelial cells (51) that are in contact with the basal lamina, whereas phalloidin decorates the apical microvilli and the cell attachments throughout their length (52). Compared to the above markers, AgMMP1-specific staining along the cell attachment sites was more pronounced at the midpoint (Fig. 1D).

S-MMP1 is constitutively secreted by an *A. gambiae* hemocyte-like cell line. *Anopheles* hemocyte-like cells have been previously proven to be useful in molecular/biochemical studies of hemocyte-specific proteins overcoming the limited availability of mosquito hemolymph (43–45). Western blot analysis of cell pellet (CP) and culture medium (CM) of such a hemocyte-like cell line, Sua 4.0, revealed an abundant presence of S-MMP1 in the CM of cells treated with *GFP*-dsRNA for 2 or 3 days, which was diminished in the CM of cells treated with *AgMMP1*-dsRNA for the same period (Fig. 1E, left, black stars). In addition to the abundant presence of the zymogen S-MMP1 in the CM of Sua 4.0 cells, a faint band corresponding to the size of zymogen MT-MMP1 was detected only in the CP of *GFP*-dsRNA treated cells (Fig. 1E, left, black arrowhead). It should be stressed that Sua 4.0 is not a clonal cell line; thus, detection of both S-MMP1 and MT-MMP1 may indicate coexistence of different cell types. Nevertheless, the predominant presence of S-MMP1 suggests that most of the Sua 4.0 cells possess a hemocyte-like identity.

Casein zymography of Sua 4.0 CM revealed the presence of two lytic bands, one with a molecular mass corresponding to the mass of the zymogen S-MMP1 (~55 kDa) and a smaller one (~45 kDa). Both bands were present only in the CM of the *GFP* dsRNA-treated cells and absent from the CM of *AgMMP1* dsRNA-treated cells suggesting that both activities are AgMMP1 related (Fig. 1E, middle panel). The size difference of the two bands suggests that the 45-kDa protein might correspond to the active form of S-MMP1; however, we cannot exclude the possibility that it might represent an alternative S-MMP1 degradation product. Western analysis of the same samples used in casein zymography verified the presence of the ~45-kDa band in the CM of the *GFP* dsRNA-treated cells, which was not previously detected by Western blotting in Sua 4.0 cell supernatants or in hemolymph extracts (Fig. 1E, middle panel, pair of black stars). One possible explanation is that CM protein precipitation, omission of β-mercaptoethanol from the loading buffer, and/or avoiding boiling of the samples, as

is required in the case of zymography, allows in tube cleavage/maturation of the zymogen S-MMP1, either by autoproteolysis or by another unknown protease.

Ectopic expression of an activated MT-MMP1 in Sua 4.0 cells results in increased self-proteolysis. In order to have an efficient and controllable system to produce MT-MMP1, we expressed the protein in Sua 4.0 cells. Initial experiments using the entire cDNA encoding the complete protein were unsuccessful, as only the zymogen MT-MMP1 was produced (data not shown), a result which verified Sua 4.0 cells' incompetence to process AgMMP1s into their active forms possibly due to the lack of related ER-resident proteases (e.g., furin). Thus, in a next step, we constructed an "activated" MT-MMP1 form (aMT-MMP1), in which the signal peptide and the prodomain were replaced by a1AT signal sequence and a three-myc epitope tag (3xmyc) (Fig. 2A). This activated MT-MMP1 artificial gene was placed under a promoter regulated by the presence of tetracycline-dependent transactivators, and expression was achieved through its cotransfection with a plasmid expressing the rtTA transactivator under the control of the constitutive actin 5C promoter.

Cell extracts (CP) and culture supernatants (CM) of the transfected cells were subjected to Western analysis. Strikingly, although no protein product with the expected molecular mass for the intact aMT-MMP1 (~63 kDa) was detected with the anti-AgMMP1 serum, two new AgMMP1 "species" were apparent in the extracts of transfected cells; an ~42 kDa protein detected in the cell pellet (CP), and an ~34-kDa protein prominent in the culture medium (CM) (Fig. 2A, bottom panel, aMT-MMP1, black and gray arrowheads, respectively). On the other side, no changes in the endogenous S-MMP1 levels were observed (Fig. 2A, bottom panel, black star).

Treatment of the cells upon transfection with the metalloprotease small-molecule inhibitor GM6001, or cotransfection of the aMT-MMP1 and AgTIMP, resulted in a significant reduction of the relative amounts of the above two protein products (Fig. 2B; see Fig. S2A in the supplemental material) and in a slight increase of the intact aMT-MMP1, detected only by an anti-myc antibody (Fig. 2B, a-myc, and Fig. S2A).

The failure to detect intact aMT-MMP1 with the anti-AgMMP1 antibody suggests that upon its expression in Sua 4.0 cells, aMT-MMP1 is rapidly processed into the 42-kDa and 34-kDa proteolytic products. Susceptibility of this proteolytic processing to GM6001 and AgTIMP inhibition further suggests that is due to self-proteolysis. Strikingly, one of the proteolytic fragments (34 kDa) has a similar molecular mass with the MMP1-related product occasionally detected in the midgut extracts (compare Fig. 2A, gray arrowhead, CM and MG extracts). Proteolytic derivatives have been previously identified for several MMPs, either *in vivo* or *in vitro* (53) derived from self-proteolysis promoted by overexpression and/or protein aggregation (54, 55). Mosquito cell lines could offer a manageable toolbox to further study posttranslational regulation of *Anopheles* MMPs as in the case mentioned above.

Blood feeding and/or parasite infection induce rapid changes in MT-MMP1 expression. Following blood feeding, the mosquito midgut stretches enormously in order to accommodate the blood meal, returning to its normal size only upon the completion of blood digestion. Moreover, in *Plasmodium*-infected midguts, pronounced epithelial lesions are generated as a result of ookinete invasion (52). It is thus reasonable to speculate that
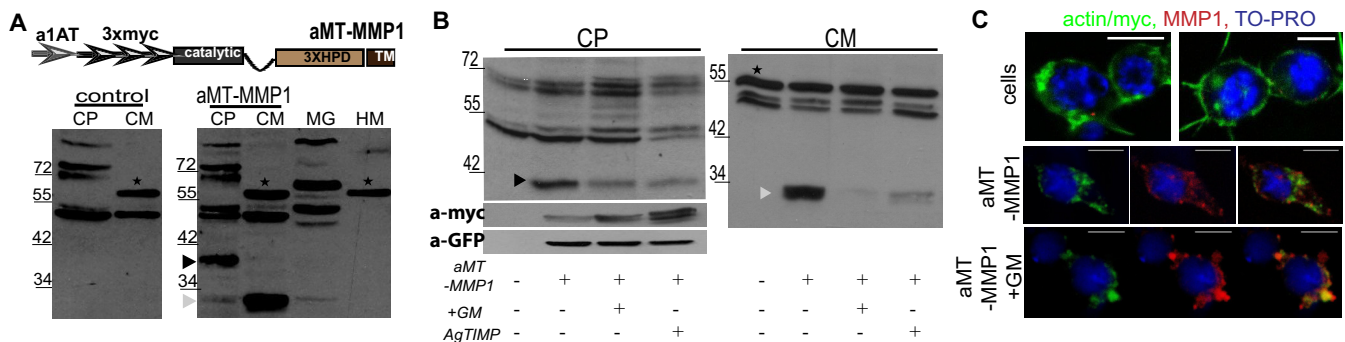
FIG 2 MT-MMP1 expression and processing in an *Anopheles* hemocyte cell line. (A, top) Schematic representation of the truncated/activated MT-MMP1 form (aMT-MMP1) ectopically expressed in Sua 4.0 cells. (Bottom) Western blot analysis of protein extracts derived from cell pellets (CP) and culture medium (CM) of Sua 4.0 cells transiently transfected with plasmids expressing aMT-MMP1. The black star indicates the position of endogenously expressed precursor S-MMP1; the black and gray arrowheads indicate the positions of the 42-kDa and 34-kDa aMT-MMP1-related protein products detected in the CP and CM, respectively, of the transfected cells. (B) Effect of the metalloprotease inhibitor GM6001 and/or AgTIMP on the generation of 42-kDa and 34-kDa aMT-MMP1 proteolytic products. Sua 4.0 cells were transfected with a plasmid expressing aMT-MMP1 and subsequently treated with the GM6001 inhibitor or transfected with a combination of plasmids expressing aMT-MMP1 and AgTIMP. In either case, the levels of 42-kDa product in the CP are reduced, while in parallel, the levels of unprocessed aMT-MMP1 are increased (as revealed with the anti-myc antibody [a-myc]), although the transfection efficiency was the same, as revealed by GFP expression (anti-GFP [a-GFP]). Similarly, the levels of the 34-kDa product are severely reduced in the CM upon GM6001 treatment or in the presence of AgTIMP inhibitor (right panel). Quantitative densitometry of three Western blots (deriving from three independent experiments, including the ones presented here) is shown in Fig. S2A in the supplemental material. (C) IFAs of untransfected Sua 4.0 cells (top row) and of Sua 4.0 cells transfected with plasmid expressing aMT-MMP1 left untreated (middle row) or treated with the GM6001 inhibitor (bottom row). Transfected cells were stained with anti-myc antibody (Ab) that reveals only the intact aMT-MMP1 and anti-AgMMP1 purified serum. Notice that the colocalization of myc and AgMMP1 is more pronounced upon treatment with the GM6001 inhibitor. The cells were stained with phalloidin or anti-myc (green), anti-AgMMP1 (red), and TO-PRO (blue). Bars, 5 μm.

physiological changes in the course of these two processes might reflect on alterations in the *AgMMP1* gene expression.

We used quantitative reverse transcription-PCR (qRT-PCR) in order to monitor the *AgMMP1* transcript levels in the midgut at three different time points (24 h, 48 h, and 96 h) postfeeding (PF) on an uninfected (control) or a *Plasmodium berghei*-infected (infected) mouse. For each time point and each condition (control/infected), expression of *AgMMP1* was compared to expression of the transcript in midguts isolated within a few minutes PF. In the following text we call this sample MPF. Twenty-four hours after the ingestion of blood (24 h control), the levels of *AgMMP1* transcript were found reduced (~0.7-fold; $P > 0.05$) compared to the level of transcript at the MPF control time point. In striking contrast, 24 h upon the uptake of an infected-blood meal (24 h infected), the levels of *AgMMP1* transcripts were ~3-fold induced ($P < 0.001$) compared to the levels recorded at the corresponding MPF time point (Fig. 3A).

As the time after blood ingestion advances, *AgMMP1* transcript levels start to increase in the naive-blood-fed midguts (48 h control), while they start to decrease in the infected midguts (48 h infected), so that 4 days after uptake of the blood meal, *AgMMP1* transcript levels approximate those recorded at the MPF time points (MPF control/infected). Parallel qRT-PCR analysis of the same samples monitoring the changes in *AgTIMP* gene expression revealed that 24 h after an infected-blood meal the levels of *AgTIMP* transcript also show a slight increase (~2.08-fold; $P < 0.01$) relative to the level at the MPF time point (Fig. 3B).

Changes in total MT-MMP1 protein levels in extracts of naive-blood-fed midguts prepared in parallel were in accordance with those of the *AgMMP1* transcript (Fig. 4A, left and middle panels; see Fig. S2B in the supplemental material). The band corresponding to the zymogen MT-MMP1 (Fig. 4A, black arrowhead, and Fig. S2B, top left graph) is reduced at 24 h PF, emerging again 3 days later (96 h, control), further suggesting that *de novo* synthesis
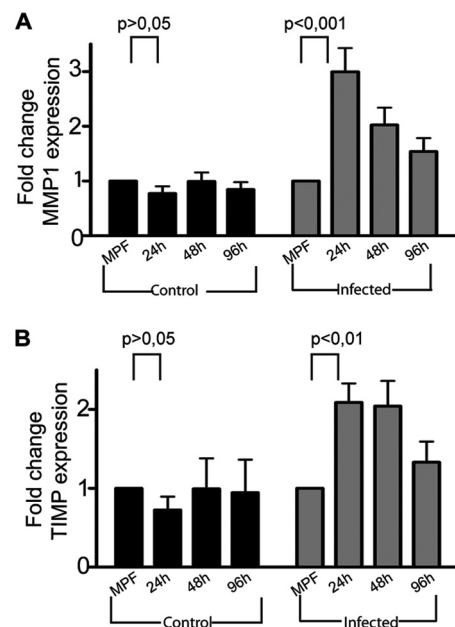

FIG 3 Expression profile of *AgMMP1* and *AgTIMP* in the midgut postfeeding. (A and B) Relative expression of *AgMMP1* (A) and *AgTIMP* (B) transcripts at 24, 48, and 96 h postfeeding on blood from a healthy mouse (control) or a *P. berghei*-infected mouse was determined by real-time PCR using the standard curve method for quantification. Data are presented as fold change in the expression of each transcript relative to the MPF (minutes postfeeding) time point (for each situation, the fold change in the level of expression of transcript in the control to the level of expression in the infected mouse). In all cases, samples were normalized against the ribosomal protein S7 transcripts. Values are means ± standard errors (SE) (error bars) from four independent experiments. Statistical significance was determined using two-way analysis of variance (ANOVA) followed by Bonferroni's posttest to compare individual data sets to the controls.
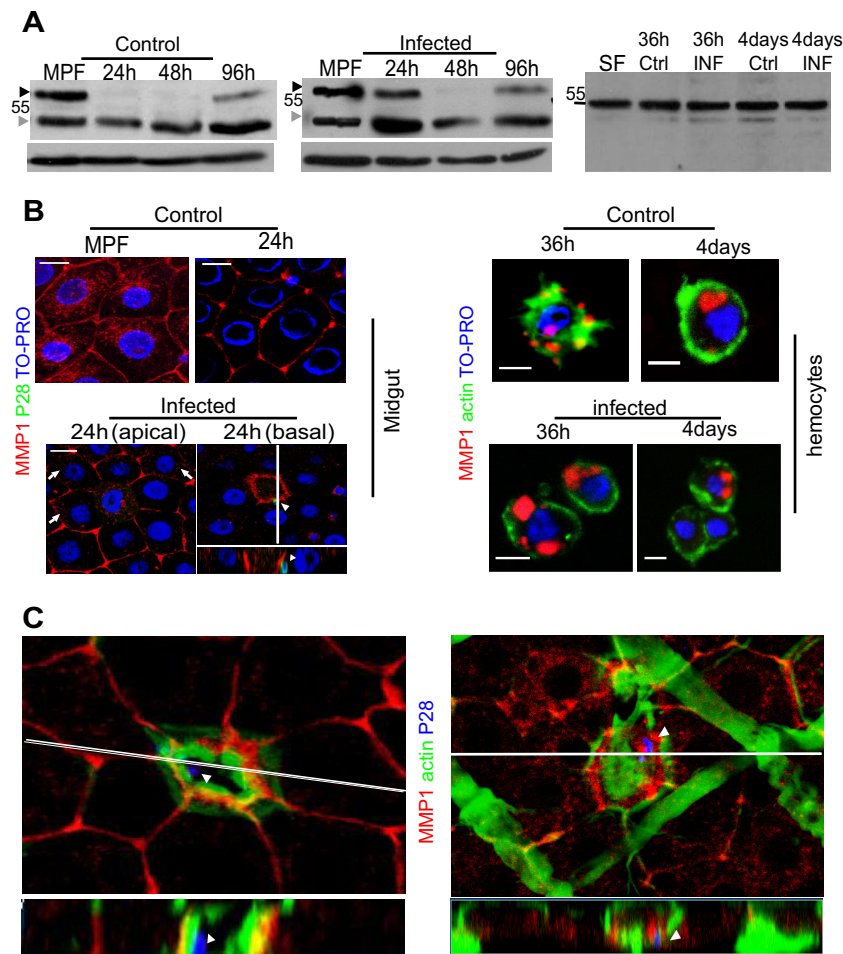
FIG 4 AgMMP1 processing and subcellular localization upon blood feeding and/or infection. (A, left and middle) Western blot analysis of total mosquito midgut proteins extracted at the same time points after feeding on a healthy mouse (control) or an infected mouse, probed with anti-AgMMP1 serum. The positions of MT-MMP1 zymogen and active forms are indicated by black and gray arrowheads, respectively. Samples were normalized against tubulin (bottom blot in both cases). (Right) Western analysis of total hemolymph proteins extracted at 36 h and 4 days PF (control [Ctrl] and infected [INF]) probed with the anti-AgMMP1 purified serum. Total hemolymph protein extract from sugar-fed female mosquitoes (SF) is shown. All hemolymph extracts were normalized by the Bradford assay prior to loading (∼70 μg). Quantitative densitometry for both midgut and hemolymph Western blots (three Western blots derived from three independent experiments, including the ones presented here) is shown in Fig. S2B and S2C, respectively, in the supplemental material. (B, left) IFAs of midgut epithelia stained with anti-AgMMP1 serum. (Left top) Stacks of horizontal optical sections (apical to middle plane) from epithelial IFAs isolated at two time points, MPF (left) and 24 h (right) PF with noninfected blood (control). (Left bottom) Merged horizontal optical sections of a selected ookinete invasion site in an infected midgut 24 h PF; (left) stack of apical to middle optical sections revealing a characteristic rosette formed by the cells neighboring the invaded healthy cells. White arrows mark cytoplasmic dots. (Right) Stack of middle to basal optical sections of the same ookinete invasion site revealing the ring evident at the basal site of the epithelium formed by the local aggregation of MT-MMP1. The white arrowheads indicate the positions of the ookinete. *xz* vertical projection was reconstructed perpendicular to the white line and is shown in the bottom panel. (Right) IFAs of peripheral hemocytes isolated at the indicated time points (36 h and 4 days) from control and infected female mosquitoes stained with AgMMP1 purified serum (red), TO-PRO (blue), or P28 (ookinete surface protein)/phalloidin (hemocytes) (green). Bars, 10 μm (midgut epithelia) and 5 μm (hemocytes). (C) Stacks of horizontal optical sections (basal) of two randomly selected ookinete invasion sites. The MT-MMP1 ring (red) is located between an actin ring or cone formed at the base of the invaded cell and an outer actin ring formed at the margins of the neighboring healthy cells; *xz* vertical optical cross sections were reconstructed perpendicular to the white line and are shown in the bottom panel. The white arrowheads indicate the ookinetes in both cases. The cells were stained with phalloidin (green), AgMMP1 (red), and P28 (blue). Magnification, ×100.

of MT-MMP1 is reduced within this time interval. Similarly, total MT-MMP1 protein levels mirrored those of the *AgMMP1* transcript at the selected time points upon infected-blood meal ingestion, showing a considerable increase at 24 h postfeeding on *P. berghei*-infected mouse (Fig. S2B, bottom graph). In striking contrast to its reduction 24 h postfeeding on a healthy mouse, zymogen MT-MMP1 is detected in *Plasmodium*-infected midgut extracts at the same time point and at levels comparable to those detected in isolated midgut extracts from the corresponding MPF

time point (Fig. 4A, middle panel, black arrowhead, and Fig. S2B, top left graph). Moreover, at the 24 h infected time point, the levels of processed MT-MMP1 showed a significant increase compared to the level at the MPF infected time point, suggesting a concomitant accelerated maturation of MT-MMP1 to its active form (Fig. 4A, middle panel, gray arrowhead, and Fig. S2B, top right graph).

Twenty-four hours upon the ingestion of an infected-blood meal, the majority of *Plasmodium* ookinetes have completed their

differentiation in the midgut lumen and massively penetrate the mosquito midgut epithelium; hence, induction of *AgMMP1* expression and accelerated MT-MMP1 maturation mark the process.

Dynamic changes of MT-MMP1 subcellular localization are recorded during naive-blood feeding and infection. Staining with anti-AgMMP1 serum of midgut sheets dissected immediately after the uptake of blood and 24 h later have also revealed a dynamic pattern of MT-MMP1 subcellular distribution. Independently of the parasite's presence, a few minutes postfeeding, MT-MMP1 staining is evident both at the cytoplasm and the borders of the midgut epithelial cells (Fig. 4B, top left). Twenty-four hours postfeeding on blood from a healthy mouse, the signal was more clearly detected in the cell attachments (Fig. 4B, top right), whereas in infected midguts at the same time point, anti-AgMMP1 serum stains both the cytoplasm in a weak dot pattern and the cell attachments (Fig. 4B, bottom left, arrows indicate cytoplasmic dots), in agreement with the presence of both zymogen and active MT-MMP1 forms in the corresponding protein extracts. Most importantly, IFAs of infected midguts revealed AgMMP1 depicted rosettes, at the apical side (Fig. 4B, bottom left) coupled to AgMMP1 rings evident at the basal side in close association with the invading ookinetes (Fig. 4B, bottom right).

The cellular events taking place at the ookinete invasion sites have been well described. Invaded midgut cells are ultimately destroyed and quickly removed from the epithelium. The integrity of the midgut tissue is quickly restored through the active engagement of the cells neighboring the invaded cells that elongate to fill the gap (52). This healing process can be visualized by phalloidin staining that also depicts rosettes formed by the borders of the elongated neighboring cells associated with two actin rings, an inner actin ring (or sometimes an actin mass) formed at the base of the invaded cell and an outer actin ring formed at the leading edges of the neighboring cells. Costaining experiments with anti-AgMMP1 serum and phalloidin confirmed an increased accumulation of AgMMP1 between those two rings (Fig. 4C).

In order to investigate whether the presence of the parasite induces any qualitative/quantitative changes in AgMMP1 expression in the hemocytes, hemolymph extracts obtained at two different time points postfeeding (at 36 h and at 4 days) on blood from a healthy mouse or an infected mouse were analyzed by Western blotting. At 36 h after infection, invading ookinetes reach the basal lamina and start their differentiation into oocysts, whereas at 4 days after infection, they are already transformed into developing oocysts that rest in the basal labyrinth of the midgut epithelium in contact with the hemolymph. Our analysis revealed that the levels of zymogen S-MMP1 are comparable between naive- and/or infected-blood-fed and sugar-fed (control) mosquitoes (Fig. 4A, right panel; see Fig. S2C in the supplemental material) at the selected time points, while IFAs of peripheral hemocytes did not reveal any deviation from the characteristic S-MMP1 granular staining pattern (Fig. 4B, right panels).

AgMMP1 acts as an agonist of *Plasmodium* oocyst development. Changes in the MT-MMP1 expression profile recorded in the course of ookinete midgut invasion prompted us to investigate the effect of AgMMP1 depletion on *Plasmodium* sporogonic development. Female mosquitoes from the same cohort were injected with dsRNA specific for *AgMMP1* (*AgMMP1* dsRNA-injected [MMP1inj] group) or for *GFP* (*GFP* dsRNA-injected [GFPinj] group [control]). For each MMP1inj group, efficient silencing of *AgMMP1* was confirmed in randomly selected individuals (Fig. 5A). Only experimental sets in which we recorded a significant reduction at the expression levels of AgMMP1 were included in our analysis.

Three days after dsRNA treatment, the two mosquito groups were allowed to feed on blood from the same mouse infected with the *P. berghei* strain 507 cl1, expressing GFP throughout the life cycle (42), and the number of oocysts was monitored 7 days later. In five independent experimental sets, a significant ~4.5-fold reduction ($P < 0.001$ by the Mann-Whitney U test) in the median numbers of oocysts was recorded in the mosquitoes depleted for AgMMP1 compared to the control group (Fig. 5B, left; see Table S1 in the supplemental material). Due to the subcellular distribution of MT-MMP1 in infected midguts 24 h PF, we investigated the process of epithelial healing upon protease silencing using two available cellular markers, actin and integrin. The formation of actin rings and the characteristic rosettes and the masking of invading ookinetes by integrin were not affected by AgMMP1 depletion (Fig. 5B, right panels, white arrowheads). Moreover, no increased death rate was observed in the *AgMMP1* dsRNA-injected group compared to the control group, suggesting that epithelial healing is not affected.

In order to differentiate between an effect of AgMMP1 depletion on ookinete midgut invasion or at a later point during oocyst development, the experiment was repeated in exactly the same way, but this time oocyst counting was performed in randomly selected mosquitoes at two different time points after infection (2 and 7 days). Two days after infection, the majority of successfully invading ookinetes have reached the basal lamina and have started their differentiation into young oocysts, as is evidenced by morphological changes (rounding up) and the expression of an oocyst diagnostic marker, namely, PbCap380 (50). Seven days after infection, oocyst development has progressed considerably, and oocysts are easily identified due to their increased size and intense GFP fluorescence (Fig. 5C, left, insets).

Three independent experiments revealed that *AgMMP1* silencing does not significantly affect the midgut invasion process, since the numbers of parasites that have begun differentiating into oocysts (PbCap380 positive) were similar between the MMP1inj and GFPinj groups. On the contrary, 7 days after infection, the median number of oocysts recorded in MMP1inj mosquitoes showed the same drastic reduction as in the control group (3.14-fold; $P < 0.0005$ by pairwise Mann-Whitney test) (Fig. 5C, left; see Table S3 in the supplemental material), suggesting an agonistic function of AgMMP1 during the course of oocyst development.

A possible agonistic role of AgMMP1 (or AgMMP1-derived peptides) over oocyst development is compatible with the observation that anti-AgMMP1 serum decorates the surfaces of a number of young oocysts (3 to 4 days postinfection) (Fig. 5C, right). This number was variable in different experiments. Oocyst losses observed in the AgMMP1-depleted mosquitoes were not directly compared with the number of oocysts found positive for AgMMP1, since we cannot exclude the possibility that the AgMMP1-related product might attach to the surfaces of a greater number of oocysts undetectable by IFA.

A similar surface staining with the anti-AgMMP1 serum was not observed in invading ookinetes (data not shown) or in late oocysts (7 to 10 days old) (Fig. 5C, right). Moreover, oocysts in *AgMMP1* dsRNA-treated mosquitoes lacked similar staining
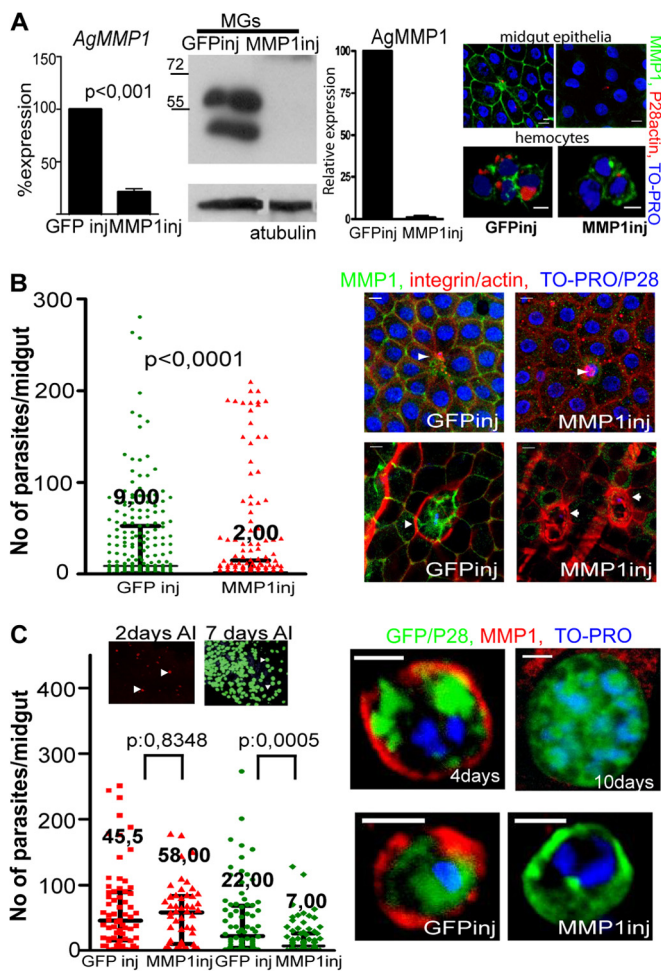
FIG 5 Effect of *AgMMP1* silencing on *Plasmodium* sporogonic development. (A) Verification of *AgMMP1* gene silencing. (Left) qRT-PCR transcript quantification of *AgMMP1* in isolated midguts (MGs) of *AgMMP1* dsRNA-injected (MMP1inj) mosquitoes; transcript levels are shown as percent abundance relative to level of expression of transcripts in the respective control mosquitoes (GFP dsRNA injected [GFPinj]). Transcript levels of the ribosomal protein S7 were used for cDNA sample normalization. Values are means plus standard errors (SE) (error bars) from three independent biological experiments. Statistical significance was determined using the Student *t* test. (Middle left) A representative Western blot probed with anti-AgMMP1 of midgut extracts derived from mosquitoes injected with *AgMMP1* dsRNA compared to extracts derived from sibling mosquitoes injected with *GFP* dsRNA (control). (Middle right) Quantitative densitometry of expression of AgMMP1 in the dsRNA-injected mosquitoes. Samples were normalized using tubulin. Expression in MMP1inj mosquitoes is presented as a percentage relative to the value for the control (set at 100%). The difference in expression is statistically significant ($P < 0.001$ by Student's *t* test). (Right) IFAs from midgut epithelia and peripheral hemocytes derived from *dsMMP1* and *dsGFP* RNA-treated mosquitoes stained with anti-AgMMP1 purified serum (green), phalloidin or anti-P28 (red), or TO-PRO (blue). Note the absence of AgMMP1 staining in *dsMMP1* RNA-treated samples. Bars, 10 μm (midgut epithelia) or 5 μm (hemocytes). (B, left) Graphical illustration of the infection intensity (measured as number of oocysts at 7 days postinfection) in *P. berghei*-infected female mosquitoes injected with dsRNA specific for *AgMMP1* compared to control mosquitoes (GFPinj). Each dot represents the number of oocysts from the midgut of an individual mosquito. The horizontal lines indicate the median numbers of oocysts. Error bars represent the interquartile range. The values found in the infection experiments are provided in Table S1 in the supplemental material. Statistical significance was determined using the Mann-Whitney U test. (Right) Stacks of horizontal optical sections (basal) of randomly selected ookinete invasion sites of midgut epithelia derived from either the GFPinj or MMP1inj group. Epithelia are stained with anti-AgMMP1 serum and anti-

integrin beta subunit (top panel) or phalloidin (bottom panel). Arrowheads indicate the presence of invading ookinetes in both cases. The cells were stained with integrin/actin (red), AgMMP1 (green), or TO-PRO/P28 (blue). Bars, 10 μm. (C, right) Oocysts counted in midguts of female mosquitoes depleted for AgMMP1 or injected with dsGFP RNA (control) at two different time points after infection, 2 days after infection (AI) (early oocysts revealed with PbCap380 staining [red]) and 7 days AI (revealed by GFP expression and size [green]). (Insets) Characteristic midgut for each time point of MMPinj mosquitoes. The white arrowheads indicate PbCap380-stained and GFP-expressing oocysts, respectively. The median numbers of oocysts in each case are indicated. Error bars represent the interquartile range. Statistical significance was determined using pairwise Mann-Whitney U test ($P = 0.8348$ or $P < 0.0005$). The results of the experiments are provided in Table S3 in the supplemental material. (Right top) Confocal pictures of early (4 days) and late (10 to 12 days) oocysts stained with the anti-AgMMP1 purified serum. Only a subset of early oocysts stains intensely. (Right bottom) AgMMP1 early oocyst surface staining is never observed in female mosquitoes depleted for AgMMP1 (MMP1inj). The cells were stained with AgMMP1 (red), P28 (early oocysts) or endogenous GFP (late oocysts) (green), or TO-PRO (blue). Bars, 3 μm.

(Fig. 5C, MMP1inj). Therefore, the possibility of a technical artifact can be excluded.

We attempted to reveal AgMMP1 activity on the surfaces of young oocysts by performing *in situ* zymography; however, our efforts were hindered by the very high protease content of the midgut (data not shown). Additionally, in order to reveal whether the proteolytic activity of AgMMP1 is responsible for its protective role during parasite development in the mosquito, similar experiments were performed for the inhibitor of MMPs, *AgTIMP*. In this case, one would expect a statistically significant increase in the oocyst burden. In contrast, we recorded a slight 2.3-fold increase ($P = 0.1261$ by Mann-Whitney U test) in the oocyst numbers of the AgTIMPinj mosquitoes, compared to the control GFPinj mosquitoes (see Fig. S3 and Table S2 in the supplemental material). These results were inconclusive regarding the importance of AgMMP1 proteolytic activity in the development of the parasite for two reasons. First of all, the surfaces of young oocysts are not stained by an anti-AgTIMP purified serum in IFAs (see Fig. S3B in the supplemental material). This could imply that AgTIMP expression levels are not high enough to inhibit AgMMP1 in the vicinity of the parasite. Moreover, the phenotype of AgTIMP silencing might also have implications for AgMMP2 (Fig. S3C) and AgMMP3 in parasite development, since it is an efficient inhibitor of all three metalloproteases of the mosquito, as supported by its homologues in *Drosophila* and *Tribolium* (7, 56).

DISCUSSION

The gene deposited in Anobase with the accession number AGAP006904 encodes a protein structurally defined as a matrix metalloprotease (MMP) and thus was named *AgMMP1*. We showed that AgMMP1 is expressed in two alternative isoforms, a transmembrane/membrane type (MT-MMP1) and a secreted (S-MMP1) one, encoded from alternatively spliced transcripts. In mammals, membrane type and secreted MMPs are encoded by different genes; however, generation of both MMP species from the same gene via alternative splicing appears to be common for arthropod MMP1 proteins (MMP1s); from the five predicted isoforms of *Drosophila* MMP1, two have been so far identified (one secreted and one membrane associated) (27).

We showed that the MT-MMP1 isoform is predominantly expressed in epithelial tissues, while the expression of S-MMP1 is restricted to hemocytes. Within peripheral hemocytes, S-MMP1

accumulates in large vesicles in the form of zymogen, which is also produced at high levels in *Anopheles* hemocyte-like Sua 4.0 cells and is constitutively secreted in the cell supernatant. Interestingly, the homologue of AgMMP1 in *Tribolium* is also shown to be expressed in hemocytes of the organism (7, 39).

The failure to detect active S-MMP1 leads to the assumption that maturation of S-MMP1 zymogen is stimulated postsecretion, as has been reported for most of the secreted MMPs (9, 10). Different ways for the postsecretion activation of MMPs have been suggested. Some MMPs have been shown to interact upon their secretion with proteoglycans or other cell surface proteins (57, 58), and this interaction results in their local aggregation and activation. MMP2 (gelatinase A) is activated at the pericellular space by the membrane type MT1-MMP through a mechanism involving the tissue inhibitor of metalloproteases TIMP2 as a "bridge" (59). MMP zymogen maturation is known to become enhanced by the presence of pathogens. Overproduced NO during microbial infections is speculated to activate secreted pro-MMPs by the chemical modification of the "cysteine switch" (60, 61); during West Nile virus (62) and *Plasmodium falciparum* (63) infection, expression of active MMP-9 was shown to increase significantly. In the case of *Plasmodium* infection, *in vitro* studies suggest a mechanism through which hemozoin provokes autocatalytic processing of the propeptide (64). It would be interesting to determine whether plasmodial proteases expressed in the sexual stages of the parasite (65) could interact with host MMPs, in this case latent S-MMP1, and mediate its activation directly or indirectly.

At this time, potential stimuli that might provoke maturation of S-MMP1 zymogen *in vivo* remain unknown; however, our results imply that *Plasmodium* infection does not lead to detectable levels of circulating active S-MMP1. In fact, a proteolytic activity with a molecular mass similar to that of the active S-MMP1 was detected in the culture medium (CM) of Sua 4.0 hemocyte-like cells only upon its processing for zymography, possibly derived from self-proteolysis of the zymogen S-MMP1 promoted by CM condensation.

Unlike S-MMP1, both forms of the MT-MMP1 were detected in the *Anopheles* midgut extracts, implying that maturation of the MT-MMP1 zymogen is mediated intracellularly possibly by ER-resident proprotein convertases (e.g., furin). During blood meal digestion and midgut infection by *Plasmodium* ookinetes, we recorded rapid changes in the MT-MMP1 transcription rate, in the ratio of MT-MMP1 zymogen/active protease, and in MT-MMP1 subcellular localization, which establish *Anopheles* MT-MMP1 as a sensitive sensor of the drastic changes in midgut physiology associated with these two processes. Enhanced MMP1 transcription and increased maturation of MT-MMP1 marked the process of ookinete midgut invasion that provokes severe destruction of the midgut epithelium. Moreover, IFAs of epithelial sheets from infected midguts revealed an increased accumulation of MT-MMP1 at the sites of ookinete invasion and at the borders of healthy cells next to invaded cells. Accumulated MT-MMP1 formed a characteristic ring, positioned between the two previously described actin rings (a purse string-like structure responsible for the expulsion of the deteriorated invaded cells from the epithelium) (52). These cytological findings are in agreement with reports showing increased MMP expression in cells surrounding a mechanically provoked wound, so as to allow the dissolution of extracellular matrix components and to facilitate the sliding of cell edges to cover the wound (66). In *Drosophila*, it was shown that MMP1 is

upregulated in the epidermal cells surrounding such wounds and that it is required for effective wound healing (32).

Yet, as in the naive mosquito midguts, actin rings and elongation of the healthy cells, forming the characteristic rosettes, as evidenced also by integrin staining, were observed in AgMMP1-depleted midguts and at almost all ookinete invasion sites, indicating that the midgut healing that follows ookinete invasion is not drastically affected. A possible time delay in the healing process due to decreased MT-MMP1 levels would be difficult to record, since invasion of ookinetes is not synchronous. Moreover, we cannot exclude the possibility that despite the lack of detectable MT-MMP1 in the dsMMP1-treated mosquitoes, sufficient amounts might be still present. Alternative ways to ensure complete depletion of AgMMP1 (e.g., *in vivo* expression of *AgMMP1* dsRNA as opposed to injected *AgMMP1* dsRNA) and monitoring the healing progression at selected invasion sites in real time might provide us with more-definitive answers regarding the functional contribution of MT-MMP1 in the midgut healing process.

Interestingly, 3 to 4 days postfeeding on blood from an infected mouse, AgMMP1 material, whose identity remains unknown at this time, is found on the surfaces of a fraction of young oocysts. Interaction of AgMMP1 with the growing oocyst can be direct, as in the case of laminin, which associates with the parasite at this developmental stage (67–69), or indirect through proteins of the extracellular matrix (70, 71). Since AgMMP1 was not detected on the basal side of the epithelium (Fig. 1D), we hypothesize two potential sources from which it could originate: the hemocytes, which are in contact with the basal lamina of the midgut epithelium and/or the ookinete midgut invasion sites at the basal side, where MT-MMP1 is accumulated. In the former case, the AgMMP1-related product might be locally secreted S-MMP1 zymogen that upon its aggregation on the oocyst surface might convert into the active S-MMP1 form, while in the latter case, it might correspond to soluble derivatives of MT-MMP1 coming from local proteolysis. Self-proteolysis promoted by MMP overexpression and/or aggregation has been suggested before as a mode of attenuation of the overwhelming MMP activity (53). In fact, an ~34-kDa protein product, susceptible to *AgMMP1* dsRNA silencing, was occasionally detected in midgut extracts, while a secreted proteolytic derivative of a similar molecular mass was also detected in the cell supernatant of Sua 4.0 cells ectopically expressing an activated version of MT-MMP1.

One of our initial assumptions was that AgMMP1 might facilitate the ookinete invasion process. This assumption was based on previous reports showing that infection by several pathogens (parasites, viruses, or bacteria) is associated with increased MMP activity in the invaded tissue, facilitating pathogen migration and/or the establishment of systemic infections (7, 62, 63, 72, 73). Indeed, the number of oocysts developing in the midguts of *AgMMP1* dsRNA-treated mosquitoes was severely reduced (in some cases 7-fold compared to the value for the control [see Table S1 in the supplemental material]). However, more-precise recordings revealed that the loss of parasites in AgMMP1-depleted mosquitoes do not correlate with a decreased midgut invasion rate but rather occur in the course of oocyst development. This phenotypic observation correlates well with the masking of young oocysts from AgMMP1-related material, supporting the hypothesis of an agonistic role of AgMMP1 during sporogonic development of the parasite.

The critical question remaining unanswered is the mechanism

through which AgMMP1 confers its agonistic role over growing oocysts. One hypothesis could be that the deposited material interacts with molecules of the mosquito immune system, thus protecting the growing oocyst, either actively or passively. A similar role was assigned to *Anopheles* lysozyme c-1, which also interacts with the surfaces of growing oocysts (74). It has been documented that the number of *P. berghei* parasites present in the midgut 24 h PF decreases gradually during the next 2 days due to immune responses (48, 75). AgMMP1 could mask the parasite from mosquito immune attacks, as has been suggested for laminin (76) and other molecules of the ECM, such as collagen (77). Additionally, the protease could process effector molecules of the innate immune system, such as antimicrobial peptides (78, 79) and the complement C3-like protein TEP1 (thioester-containing protein 1) (80), a very potent effector against bacteria and/or *P. berghei*. Interestingly, human MT1-MMP was shown to be upregulated in cancer cells and to shed activated complement C3 fragments from their surface, thus abolishing their opsonization and phagocytosis (81).

Alternatively, AgMMP1 could trigger oocyst transformation by providing the growing parasite with developmental cues that could derive from the midgut epithelium basal lamina, as is the case for human MMP-9 during angiogenesis (24). Unfortunately, very little is known regarding this stage of the parasite's life cycle. Most reports refer to metabolic needs of the parasite during sporogonic development (82–85). Although proposed (69), there are no data supporting the idea that mosquito molecules could function as developmental triggers for ookinete-to-oocyst transition. On the contrary, there have been reports showing oocyst transformation in an *in vitro* cell-free system (86).

By employing transgenesis, one could overexpress the 34-kDa MT-MMP1 proteolytic product or increase the levels of AgTIMP and S-MMP1 in the hemolymph and investigate the effect on oocyst development. Implementation of more-advanced methodologies such as transgenesis and/or proteomics will provide more-definitive answers, further increasing our knowledge regarding the function of AgMMP1 in *Anopheles* and particularly in relationship to the vector competence determination.

ACKNOWLEDGMENTS

REFERENCES

1. **Belas R, Manos J, Suvanasuthi R.** 2004. Proteus mirabilis ZapA metalloprotease degrades a broad spectrum of substrates, including antimicrobial peptides. Infect. Immun. **72:**5159–5167. http://dx.doi.org/10.1128/IAI.72.9.5159-5167.2004.
2. **Cerda-Costa N, Guevara T, Karim AY, Ksiazek M, Nguyen KA, Arolas JL, Potempa J, Gomis-Ruth FX.** 2011. The structure of the catalytic domain of Tannerella forsythia karilysin reveals it is a bacterial xenologue of animal matrix metalloproteinases. Mol. Microbiol. **79:**119–132. http://dx.doi.org/10.1111/j.1365-2958.2010.07434.x.
3. **Guyot N, Bergsson G, Butler MW, Greene CM, Weldon S, Kessler E, Levine RL, O'Neill SJ, Taggart CC, McElvaney NG.** 2010. Functional study of elafin cleaved by Pseudomonas aeruginosa metalloproteinases. Biol. Chem. **391:**705–716. http://dx.doi.org/10.1515/BC.2010.066.
4. **Ko R, Okano K, Maeda S.** 2000. Structural and functional analysis of the Xestia c-nigrum granulovirus matrix metalloproteinase. J. Virol. **74:**11240–11246. http://dx.doi.org/10.1128/JVI.74.23.11240-11246.2000.
5. **Llano E, Adam G, Pendas AM, Quesada V, Sanchez LM, Santamaria I, Noselli S, Lopez-Otin C.** 2002. Structural and enzymatic characterization of Drosophila Dm2-MMP, a membrane-bound matrix metalloproteinase with tissue-specific expression. J. Biol. Chem. **277:**23321–23329. http://dx.doi.org/10.1074/jbc.M200121200.
6. **Llano E, Pendas AM, Aza-Blanc P, Kornberg TB, Lopez-Otin C.** 2000. Dm1-MMP, a matrix metalloproteinase from Drosophila with a potential role in extracellular matrix remodeling during neural development. J. Biol. Chem. **275:**35978–35985. http://dx.doi.org/10.1074/jbc.M006045200.
7. **Knorr E, Schmidtberg H, Vilcinskas A, Altincicek B.** 2009. MMPs regulate both development and immunity in the Tribolium model insect. PLoS One **4:**e4751. http://dx.doi.org/10.1371/journal.pone.0004751.
8. **Yan C, Boyd DD.** 2007. Regulation of matrix metalloproteinase gene expression. J. Cell. Physiol. **211:**19–26. http://dx.doi.org/10.1002/jcp.20948.
9. **Ra HJ, Parks WC.** 2007. Control of matrix metalloproteinase catalytic activity. Matrix Biol. **26:**587–596. http://dx.doi.org/10.1016/j.matbio.2007.07.001.
10. **Jackson BC, Nebert DW, Vasiliou V.** 2010. Update of human and mouse matrix metalloproteinase families. Hum. Genomics **4:**194–201.
11. **Nagase H, Visse R, Murphy G.** 2006. Structure and function of matrix metalloproteinases and TIMPs. Cardiovasc. Res. **69:**562–573. http://dx.doi.org/10.1016/j.cardiores.2005.12.002.
12. **Fjeldstad K, Kolset SO.** 2005. Decreasing the metastatic potential in cancers–targeting the heparan sulfate proteoglycans. Curr. Drug Targets **6:**665–682. http://dx.doi.org/10.2174/1389450054863662.
13. **Giannelli G, Falk-Marzillier J, Schiraldi O, Stetler-Stevenson WG, Quaranta V.** 1997. Induction of cell migration by matrix metalloprotease-2 cleavage of laminin-5. Science **277:**225–228. http://dx.doi.org/10.1126/science.277.5323.225.
14. **Pal-Ghosh S, Blanco T, Tadvalkar G, Pajoohesh-Ganji A, Parthasarathy A, Zieske JD, Stepp MA.** 2011. MMP9 cleavage of the beta4 integrin ectodomain leads to recurrent epithelial erosions in mice. J. Cell Sci. **124:**2666–2675. http://dx.doi.org/10.1242/jcs.085480.
15. **Chen P, Abacherli LE, Nadler ST, Wang Y, Li Q, Parks WC.** 2009. MMP7 shedding of syndecan-1 facilitates re-epithelialization by affecting alpha(2)beta(1) integrin activation. PLoS One **4:**e6565. http://dx.doi.org/10.1371/journal.pone.0006565.
16. **McGuire JK, Li Q, Parks WC.** 2003. Matrilysin (matrix metalloproteinase-7) mediates E-cadherin ectodomain shedding in injured lung epithelium. Am. J. Pathol. **162:**1831–1843. http://dx.doi.org/10.1016/S0002-9440(10)64318-0.
17. **Martins VL, Caley M, O'Toole EA.** 2013. Matrix metalloproteinases and epidermal wound repair. Cell Tissue Res. **351:**255–268. http://dx.doi.org/10.1007/s00441-012-1410-z.
18. **Kessenbrock K, Plaks V, Werb Z.** 2010. Matrix metalloproteinases: regulators of the tumor microenvironment. Cell **141:**52–67. http://dx.doi.org/10.1016/j.cell.2010.03.015.
19. **Lauwaet T, Oliveira MJ, Mareel M, Leroy A.** 2000. Molecular mechanisms of invasion by cancer cells, leukocytes and microorganisms. Microbes Infect. **2:**923–931. http://dx.doi.org/10.1016/S1286-4579(00)00394-4.
20. **Butler GS, Overall CM.** 2009. Updated biological roles for matrix metalloproteinases and new "intracellular" substrates revealed by degradomics. Biochemistry **48:**10830–10845. http://dx.doi.org/10.1021/bi901656f.
21. **Morrison CJ, Butler GS, Rodriguez D, Overall CM.** 2009. Matrix metalloproteinase proteomics: substrates, targets, and therapy. Curr. Opin. Cell Biol. **21:**645–653. http://dx.doi.org/10.1016/j.ceb.2009.06.006.
22. **Hua H, Li M, Luo T, Yin Y, Jiang Y.** 2011. Matrix metalloproteinases in tumorigenesis: an evolving paradigm. Cell. Mol. Life Sci. **68:**3853–3868. http://dx.doi.org/10.1007/s00018-011-0763-x.
23. **Page-McCaw A, Ewald AJ, Werb Z.** 2007. Matrix metalloproteinases and the regulation of tissue remodelling. Nat. Rev. Mol. Cell Biol. **8:**221–233. http://dx.doi.org/10.1038/nrm2125.
24. **Hamano Y, Zeisberg M, Sugimoto H, Lively JC, Maeshima Y, Yang C, Hynes RO, Werb Z, Sudhakar A, Kalluri R.** 2003. Physiological levels of tumstatin, a fragment of collagen IV alpha3 chain, are generated by MMP-9 proteolysis and suppress angiogenesis via alphaV beta3 integrin. Cancer Cell **3:**589–601. http://dx.doi.org/10.1016/S1535-6108(03)00133-8.
25. **Bond ND, Nelliot A, Bernardo MK, Ayerh MA, Gorski KA, Hoshizaki DK, Woodard CT.** 2011. ssFTZ-F1 and Matrix metalloproteinase 2 are

required for fat-body remodeling in Drosophila. Dev. Biol. **360:**286–296. http://dx.doi.org/10.1016/j.ydbio.2011.09.015.

26. **Glasheen BM, Robbins RM, Piette C, Beitel GJ, Page-McCaw A.** 2010. A matrix metalloproteinase mediates airway remodeling in Drosophila. Dev. Biol. **344:**772–783. http://dx.doi.org/10.1016/j.ydbio.2010.05.504.

27. **Page-McCaw A, Serano J, Sante JM, Rubin GM.** 2003. Drosophila matrix metalloproteinases are required for tissue remodeling, but not embryonic development. Dev. Cell **4:**95–106. http://dx.doi.org/10.1016/S1534-5807(02)00400-8.

28. **McClure KD, Sustar A, Schubiger G.** 2008. Three genes control the timing, the site and the size of blastema formation in Drosophila. Dev. Biol. **319:**68–77. http://dx.doi.org/10.1016/j.ydbio.2008.04.004.

29. **Lee SH, Park JS, Kim YS, Chung HY, Yoo MA.** 2012. Requirement of matrix metalloproteinase-1 for intestinal homeostasis in the adult Drosophila midgut. Exp. Cell Res. **318:**670–681. http://dx.doi.org/10.1016/j.yexcr.2012.01.004.

30. **Miller CM, Page-McCaw A, Broihier HT.** 2008. Matrix metalloproteinases promote motor axon fasciculation in the Drosophila embryo. Development **135:**95–109.

31. **Mitten EK, Jing D, Suzuki Y.** 2012. Matrix metalloproteinases (MMPs) are required for wound closure and healing during larval leg regeneration in the flour beetle, Tribolium castaneum. Insect Biochem. Mol. Biol. **42:**854–864. http://dx.doi.org/10.1016/j.ibmb.2012.08.001.

32. **Stevens LJ, Page-McCaw A.** 2012. A secreted MMP is required for reepithelialization during wound healing. Mol. Biol. Cell **23:**1068–1079. http://dx.doi.org/10.1091/mbc.E11-09-0745.

33. **Altincicek B, Linder M, Linder D, Preissner KT, Vilcinskas A.** 2007. Microbial metalloproteinases mediate sensing of invading pathogens and activate innate immune responses in the lepidopteran model host Galleria mellonella. Infect. Immun. **75:**175–183. http://dx.doi.org/10.1128/IAI.01385-06.

34. **Parks WC, Wilson CL, Lopez-Boado YS.** 2004. Matrix metalloproteinases as modulators of inflammation and innate immunity. Nat. Rev. Immunol. **4:**617–629. http://dx.doi.org/10.1038/nri1418.

35. **Wilson CL, Schmidt AP, Pirila E, Valore EV, Ferri N, Sorsa T, Ganz T, Parks WC.** 2009. Differential processing of alpha- and beta-defensin precursors by matrix metalloproteinase-7 (MMP-7). J. Biol. Chem. **284:**8301–8311. http://dx.doi.org/10.1074/jbc.M809744200.

36. **Ito A, Mukaiyama A, Itoh Y, Nagase H, Thogersen IB, Enghild JJ, Sasaguri Y, Mori Y.** 1996. Degradation of interleukin 1beta by matrix metalloproteinases. J. Biol. Chem. **271:**14657–14660. http://dx.doi.org/10.1074/jbc.271.25.14657.

37. **Van Den Steen PE, Wuyts A, Husson SJ, Proost P, Van Damme J, Opdenakker G.** 2003. Gelatinase B/MMP-9 and neutrophil collagenase/MMP-8 process the chemokines human GCP-2/CXCL6, ENA-78/CXCL5 and mouse GCP-2/LIX and modulate their physiological activities. Eur. J. Biochem. **270:**3739–3749. http://dx.doi.org/10.1046/j.1432-1033.2003.03760.x.

38. **McQuibban GA, Gong JH, Tam EM, McCulloch CA, Clark-Lewis I, Overall CM.** 2000. Inflammation dampened by gelatinase A cleavage of monocyte chemoattractant protein-3. Science **289:**1202–1206. http://dx.doi.org/10.1126/science.289.5482.1202.

39. **Altincicek B, Vilcinskas A.** 2008. Identification of a lepidopteran matrix metalloproteinase with dual roles in metamorphosis and innate immunity. Dev. Comp. Immunol. **32:**400–409. http://dx.doi.org/10.1016/j.dci.2007.08.001.

40. **Means JC, Passarelli AL.** 2010. Viral fibroblast growth factor, matrix metalloproteases, and caspases are associated with enhancing systemic infection by baculoviruses. Proc. Natl. Acad. Sci. U. S. A. **107:**9825–9830. http://dx.doi.org/10.1073/pnas.0913582107.

41. **Schmidt RL, Rinaldo FM, Hesse SE, Hamada M, Ortiz Z, Beleford DT, Page-McCaw A, Platt JL, Tang AH.** 2011. Cleavage of PGRP-LC receptor in the Drosophila IMD pathway in response to live bacterial infection in S2 cells. Self Nonself **2:**125–141. http://dx.doi.org/10.4161/self.17882.

42. **Janse CJ, Franke-Fayard B, Waters AP.** 2006. Selection by flow-sorting of genetically transformed, GFP-expressing blood stages of the rodent malaria parasite, Plasmodium berghei. Nat. Protoc. **1:**614–623. http://dx.doi.org/10.1038/nprot.2006.88.

43. **Muller HM, Dimopoulos G, Blass C, Kafatos FC.** 1999. A hemocyte-like cell line established from the malaria vector Anopheles gambiae expresses six prophenoloxidase genes. J. Biol. Chem. **274:**11727–11735. http://dx.doi.org/10.1074/jbc.274.17.11727.

44. **Povelones M, Waterhouse RM, Kafatos FC, Christophides GK.** 2009. Leucine-rich repeat protein complex activates mosquito complement in defense against Plasmodium parasites. Science **324:**258–261. http://dx.doi.org/10.1126/science.1171400.

45. **Levashina EA, Moita LF, Blandin S, Vriend G, Lagueux M, Kafatos FC.** 2001. Conserved role of a complement-like protein in phagocytosis revealed by dsRNA knockout in cultured cells of the mosquito, Anopheles gambiae. Cell **104:**709–718. http://dx.doi.org/10.1016/S0092-8674(01)00267-7.

46. **Applied Biosystems.** 2000. ABI PRISM 7700 sequence detection system user's manual. Applied Biosystems, Foster City, CA.

47. **Blandin S, Moita LF, Kocher T, Wilm M, Kafatos FC, Levashina EA.** 2002. Reverse genetics in the mosquito Anopheles gambiae: targeted disruption of the Defensin gene. EMBO Rep. **3:**852–856. http://dx.doi.org/10.1093/embo-reports/kvf180.

48. **Abraham EG, Pinto SB, Ghosh A, Vanlandingham DL, Budd A, Higgs S, Kafatos FC, Jacobs-Lorena M, Michel K.** 2005. An immune-responsive serpin, SRPN6, mediates mosquito defense against malaria parasites. Proc. Natl. Acad. Sci. U. S. A. **102:**16327–16332. http://dx.doi.org/10.1073/pnas.0508335102.

49. **Michel K, Budd A, Pinto S, Gibson TJ, Kafatos FC.** 2005. Anopheles gambiae SRPN2 facilitates midgut invasion by the malaria parasite Plasmodium berghei. EMBO Rep. **6:**891–897. http://dx.doi.org/10.1038/sj.embor.7400478.

50. **Srinivasan P, Fujioka H, Jacobs-Lorena M.** 2008. PbCap380, a novel oocyst capsule protein, is essential for malaria parasite survival in the mosquito. Cell. Microbiol. **10:**1304–1312. http://dx.doi.org/10.1111/j.1462-5822.2008.01127.x.

51. **Mahairaki V, Lycett G, Siden-Kiamos I, Sinden RE, Louis C.** 2005. Close association of invading Plasmodium berghei and beta integrin in the Anopheles gambiae midgut. Arch. Insect Biochem. Physiol. **60:**13–19. http://dx.doi.org/10.1002/arch.20077.

52. **Han YS, Thompson J, Kafatos FC, Barillas-Mury C.** 2000. Molecular interactions between Anopheles stephensi midgut cells and Plasmodium berghei: the time bomb theory of ookinete invasion of mosquitoes. EMBO J. **19:**6030–6040. http://dx.doi.org/10.1093/emboj/19.22.6030.

53. **Osenkowski P, Toth M, Fridman R.** 2004. Processing, shedding, and endocytosis of membrane type 1-matrix metalloproteinase (MT1-MMP). J. Cell. Physiol. **200:**2–10. http://dx.doi.org/10.1002/jcp.20064.

54. **Gingras D, Page M, Annabi B, Beliveau R.** 2000. Rapid activation of matrix metalloproteinase-2 by glioma cells occurs through a posttranslational MT1-MMP-dependent mechanism. Biochim. Biophys. Acta **1497:**341–350. http://dx.doi.org/10.1016/S0167-4889(00)00071-9.

55. **Roderfeld M, Buttner FH, Bartnik E, Tschesche H.** 2000. Expression of human membrane type 1 matrix metalloproteinase in Pichia pastoris. Protein Expr. Purif. **19:**369–374. http://dx.doi.org/10.1006/prep.2000.1259.

56. **Wei S, Xie Z, Filenova E, Brew K.** 2003. Drosophila TIMP is a potent inhibitor of MMPs and TACE: similarities in structure and function to TIMP-3. Biochemistry **42:**12200–12207. http://dx.doi.org/10.1021/bi035358x.

57. **Fedarko NS, Jain A, Karadag A, Fisher LW.** 2004. Three small integrin binding ligand N-linked glycoproteins (SIBLINGs) bind and activate specific matrix metalloproteinases. FASEB J. **18:**734–736. http://dx.doi.org/10.1096/fj.03-0966fje.

58. **Shiomi T, Inoki I, Kataoka F, Ohtsuka T, Hashimoto G, Nemori R, Okada Y.** 2005. Pericellular activation of proMMP-7 (promatrilysin-1) through interaction with CD151. Lab. Invest. **85:**1489–1506. http://dx.doi.org/10.1038/labinvest.3700351.

59. **Hernandez-Barrantes S, Toth M, Bernardo MM, Yurkova M, Gervasi DC, Raz Y, Sang QA, Fridman R.** 2000. Binding of active (57 kDa) membrane type 1-matrix metalloproteinase (MT1-MMP) to tissue inhibitor of metalloproteinase (TIMP)-2 regulates MT1-MMP processing and pro-MMP-2 activation. J. Biol. Chem. **275:**12080–12089. http://dx.doi.org/10.1074/jbc.275.16.12080.

60. **Okamoto T, Akaike T, Sawa T, Miyamoto Y, van der Vliet A, Maeda H.** 2001. Activation of matrix metalloproteinases by peroxynitrite-induced protein S-glutathiolation via disulfide S-oxide formation. J. Biol. Chem. **276:**29596–29602. http://dx.doi.org/10.1074/jbc.M102417200.

61. **Okamoto T, Akuta T, Tamura F, van Der Vliet A, Akaike T.** 2004. Molecular mechanism for activation and regulation of matrix metalloproteinases during bacterial infections and respiratory inflammation. Biol. Chem. **385:**997–1006. http://dx.doi.org/10.1515/BC.2004.130.

62. **Wang P, Dai J, Bai F, Kong KF, Wong SJ, Montgomery RR, Madri JA,**

Fikrig E. 2008. Matrix metalloproteinase 9 facilitates West Nile virus entry into the brain. J. Virol. **82**:8978–8985. http://dx.doi.org/10.1128/JVI.00314-08.

63. **Prato M, Giribaldi G, Polimeni M, Gallo V, Arese P.** 2005. Phagocytosis of hemozoin enhances matrix metalloproteinase-9 activity and TNF-alpha production in human monocytes: role of matrix metalloproteinases in the pathogenesis of falciparum malaria. J. Immunol. **175**:6436–6442. http://dx.doi.org/10.4049/jimmunol.175.10.6436.

64. **Geurts N, Martens E, Van Aelst I, Proost P, Opdenakker G, Van den Steen PE.** 2008. Beta-hematin interaction with the hemopexin domain of gelatinase B/MMP-9 provokes autocatalytic processing of the propeptide, thereby priming activation by MMP-3. Biochemistry **47**:2689–2699. http://dx.doi.org/10.1021/bi702260q.

65. **Ngwa CJ, Scheuermayer M, Mair GR, Kern S, Brugl T, Wirth CC, Aminake MN, Wiesner J, Fischer R, Vilcinskas A, Pradel G.** 2013. Changes in the transcriptome of the malaria parasite Plasmodium falciparum during the initial phase of transmission from the human to the mosquito. BMC Genomics **14**:256. http://dx.doi.org/10.1186/1471-2164-14-256.

66. **Chen P, Parks WC.** 2009. Role of matrix metalloproteinases in epithelial migration. J. Cell. Biochem. **108**:1233–1243. http://dx.doi.org/10.1002/jcb.22363.

67. **Dessens JT, Siden-Kiamos I, Mendoza J, Mahairaki V, Khater E, Vlachou D, Xu XJ, Kafatos FC, Louis C, Dimopoulos G, Sinden RE.** 2003. SOAP, a novel malaria ookinete protein involved in mosquito midgut invasion and oocyst development. Mol. Microbiol. **49**:319–329. http://dx.doi.org/10.1046/j.1365-2958.2003.03566.x.

68. **Vlachou D, Lycett G, Siden-Kiamos I, Blass C, Sinden RE, Louis C.** 2001. Anopheles gambiae laminin interacts with the P25 surface protein of Plasmodium berghei ookinetes. Mol. Biochem. Parasitol. **112**:229–237. http://dx.doi.org/10.1016/S0166-6851(00)00371-6.

69. **Arrighi RB, Hurd H.** 2002. The role of Plasmodium berghei ookinete proteins in binding to basal lamina components and transformation into oocysts. Int. J. Parasitol. **32**:91–98. http://dx.doi.org/10.1016/S0020-7519(01)00298-3.

70. **Adini A, Warburg A.** 1999. Interaction of Plasmodium gallinaceum ookinetes and oocysts with extracellular matrix proteins. Parasitology **119**(Part 4):331–336. http://dx.doi.org/10.1017/S0031182099004874.

71. **Meis JF, Wismans PG, Jap PH, Lensen AH, Ponnudurai T.** 1992. A scanning electron microscopic study of the sporogonic development of Plasmodium falciparum in Anopheles stephensi. Acta Trop. **50**:227–236. http://dx.doi.org/10.1016/0001-706X(92)90079-D.

72. **Elkington PT, O'Kane CM, Friedland JS.** 2005. The paradox of matrix metalloproteinases in infectious disease. Clin. Exp. Immunol. **142**:12–20. http://dx.doi.org/10.1111/j.1365-2249.2005.02840.x.

73. **Pina-Vazquez C, Reyes-Lopez M, Ortiz-Estrada G, de la Garza M, Serrano-Luna J.** 2012. Host-parasite interaction: parasite-derived and -induced proteases that degrade human extracellular matrix. J. Parasitol. Res. **2012**:748206. http://dx.doi.org/10.1155/2012/748206.

74. **Kajla MK, Shi L, Li B, Luckhart S, Li J, Paskewitz SM.** 2011. A new role for an old antimicrobial: lysozyme c-1 can function to protect malaria parasites in Anopheles mosquitoes. PLoS One **6**:e19649. http://dx.doi.org/10.1371/journal.pone.0019649.

75. **Gupta L, Molina-Cruz A, Kumar S, Rodrigues J, Dixit R, Zamora RE, Barillas-Mury C.** 2009. The STAT pathway mediates late-phase immunity against Plasmodium in the mosquito Anopheles gambiae. Cell Host Microbe **5**:498–507. http://dx.doi.org/10.1016/j.chom.2009.04.003.

76. **Arrighi RB, Lycett G, Mahairaki V, Siden-Kiamos I, Louis C.** 2005. Laminin and the malaria parasite's journey through the mosquito midgut. J. Exp. Biol. **208**:2497–2502. http://dx.doi.org/10.1242/jeb.01664.

77. **Gare DC, Piertney SB, Billingsley PF.** 2003. Anopheles gambiae collagen IV genes: cloning, phylogeny and midgut expression associated with blood feeding and Plasmodium infection. Int. J. Parasitol. **33**:681–690. http://dx.doi.org/10.1016/S0020-7519(03)00055-9.

78. **Shahabuddin M, Fields I, Bulet P, Hoffmann JA, Miller LH.** 1998. Plasmodium gallinaceum: differential killing of some mosquito stages of the parasite by insect defensin. Exp. Parasitol. **89**:103–112. http://dx.doi.org/10.1006/expr.1998.4212.

79. **Vizioli J, Bulet P, Hoffmann JA, Kafatos FC, Muller HM, Dimopoulos G.** 2001. Gambicin: a novel immune responsive antimicrobial peptide from the malaria vector Anopheles gambiae. Proc. Natl. Acad. Sci. U. S. A. **98**:12630–12635. http://dx.doi.org/10.1073/pnas.221466798.

80. **Blandin S, Shiao SH, Moita LF, Janse CJ, Waters AP, Kafatos FC, Levashina EA.** 2004. Complement-like protein TEP1 is a determinant of vectorial capacity in the malaria vector Anopheles gambiae. Cell **116**:661–670. http://dx.doi.org/10.1016/S0092-8674(04)00173-4.

81. **Rozanov DV, Savinov AY, Golubkov VS, Postnova TI, Remacle A, Tomlinson S, Strongin AY.** 2004. Cellular membrane type-1 matrix metalloproteinase (MT1-MMP) cleaves C3b, an essential component of the complement system. J. Biol. Chem. **279**:46551–46557. http://dx.doi.org/10.1074/jbc.M405284200.

82. **van Schaijk BC, Kumar TR, Vos MW, Richman A, van Gemert GJ, Li T, Eappen AG, Williamson KC, Morahan BJ, Fishbaugher M, Kennedy M, Camargo N, Khan SM, Janse CJ, Sim KL, Hoffman SL, Kappe SH, Sauerwein RW, Fidock DA, Vaughan AM.** 2014. Type II fatty acid biosynthesis is essential for Plasmodium falciparum sporozoite development in the midgut of Anopheles mosquitoes. Eukaryot. Cell **13**:550–559. http://dx.doi.org/10.1128/EC.00264-13.

83. **Nagaraj VA, Sundaram B, Varadarajan NM, Subramani PA, Kalappa DM, Ghosh SK, Padmanaban G.** 2013. Malaria parasite-synthesized heme is essential in the mosquito and liver stages and complements host heme in the blood stages of infection. PLoS Pathog. **9**:e1003522. http://dx.doi.org/10.1371/journal.ppat.1003522.

84. **Hino A, Hirai M, Tanaka TQ, Watanabe Y, Matsuoka H, Kita K.** 2012. Critical roles of the mitochondrial complex II in oocyst formation of rodent malaria parasite Plasmodium berghei. J. Biochem. **152**:259–268. http://dx.doi.org/10.1093/jb/mvs058.

85. **Boysen KE, Matuschewski K.** 2011. Arrested oocyst maturation in Plasmodium parasites lacking type II NADH:ubiquinone dehydrogenase. J. Biol. Chem. **286**:32661–32671. http://dx.doi.org/10.1074/jbc.M111.269399.

86. **Carter V, Nacer AM, Underhill A, Sinden RE, Hurd H.** 2007. Minimum requirements for ookinete to oocyst transformation in Plasmodium. Int. J. Parasitol. **37**:1221–1232. http://dx.doi.org/10.1016/j.ijpara.2007.03.005.